Acta Crystallographica Section F
Structural Biology and Crystallization Communications
ISSN 1744-3091

Crystallization and molecular-replacement studies of the monoclonal antibody mAbR310 specific for the (*R*)-HNE-modified protein

Sohei Ito,[a]* Emi Tatsuda,[b] Kousuke Ishino,[a] Kenichiro Suzuki,[a] Hiroshi Sakai[a] and Koji Uchida[b]

[a]Department of Food and Nutritional Sciences, Graduate School of Nutritional and Environmental Sciences, University of Shizuoka, 52-1 Yada, Suruga-Ku, Shizuoka 422-8526, Japan, and [b]Graduate School of Bioagricultural Sciences, Nagoya University, Nagoya 464-8601, Japan

Correspondence e-mail: itosohei@u-shizuoka-ken.ac.jp

Received 7 March 2006
Accepted 5 May 2006

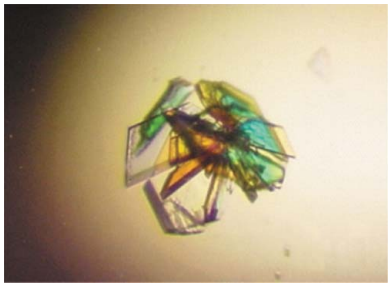

4-Hydroxy-2-nonenal (HNE), a major racemic product of lipid peroxidation, reacts with histidine to form a stable HNE–histidine Michael addition-type adduct possessing three chiral centres in the cyclic hemiacetal structure. Monoclonal antibodies against HNE-modified protein have been widely used for assessing oxidative stress *in vitro* and *in vivo*. Here, the purification, crystallization and preliminary crystallographic analysis of a Fab fragment of novel monoclonal antibody R310 (mAbR310), which recognizes (*R*)-HNE-modified protein, are reported. The Fab fragment of mAbR310 was obtained by digestion with papain, purified and crystallized. Using hanging-drop vapour-diffusion crystallization techniques, crystals of mAbR310 Fab were obtained. The crystal belongs to the monoclinic space group *C*2 (unit-cell parameters a = 127.04, b = 65.31, c = 64.29 Å, β = 118.88°) and diffracted X-rays to a resolution of 1.84 Å. The asymmetric unit contains one molecule of mAbR310, with a corresponding crystal volume per protein weight of 2.51 Å^3 Da^{-1} and a solvent content of 51.0%.

1. Introduction

Several lines of evidence indicate the oxidative modification of proteins and subsequent accumulation of modified proteins has been found in cells during aging, oxidative stress and in various pathological states, including premature diseases, muscular dystrophy, rheumatoid arthritis and atherosclerosis (Shacter, 2000; Stadtman & Levine, 2000). The important agents that give rise to the modification of a protein may be represented by lipid metabolites, such as 4-hydroxy-2-alkenals (Esterbauer *et al.*, 1991; Uchida, 2000). These metabolites are considered to be important mediators of cell damage owing to their ability to covalently modify biomolecules, which can disrupt important cellular functions and cause mutations (Esterbauer *et al.*, 1991). Furthermore, the adduction of aldehydes to apolipoprotein B in low-density lipoproteins has been strongly implicated in the mechanism by which low-density lipoprotein is converted to an atherogenic form that is taken up by macrophages, leading to the formation of foam cells (Steinberg, 1995; Steinberg *et al.*, 1989).

4-Hydroxy-2-nonenal (HNE), a reactive aldehyde, is a major product of lipid peroxidation (Benedetti *et al.*, 1980, 1986; Esterbauer *et al.*, 1982, 1991) and is believed to be largely responsible for the cytopathological effects observed during oxidative stress (Esterbauer *et al.*, 1991). The sulfhydryl groups of proteins and low-molecular-weight thiols such as glutathione (Esterbauer *et al.*, 1975), the imidazole moiety of histidine residues (Uchida & Stadtman, 1992, 1993) and the ε-amino group of lysine residues (Szweda *et al.*, 1993) are potential targets of HNE. HNE causes rapid cell death preceded by multiple pathological processes such as depletion of sulfhydryl groups, disturbances in Ca^{2+} homeostasis, inhibition of critical enzymes and disruption of protein and DNA synthesis (Esterbauer *et al.*, 1991).

We have previously raised monoclonal antibodies against HNE-modified protein. These antibodies have been used for assessing oxidative stress *in vitro* and *in vivo* (Hashimoto *et al.*, 2003; Kondo *et al.*, 2001; Okada *et al.*, 1999; Toyokuni *et al.*, 2000). Because HNE generated in lipid peroxidation is a racemic mixture of 4*R* and 4*S* enantiomers, the HNE–histidine Michael adduct possesses three

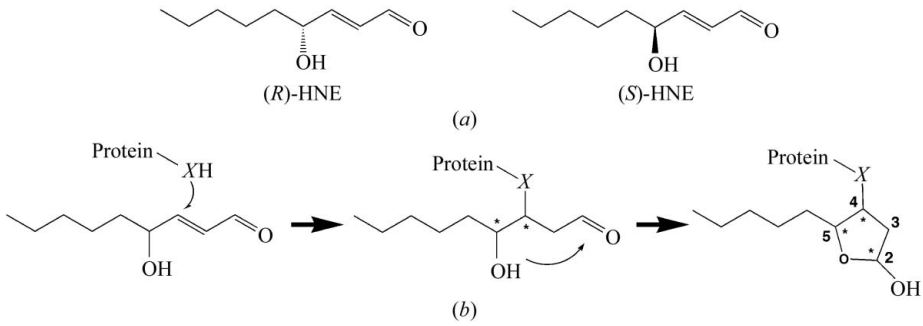

Figure 1
Reaction of (*R*,*S*)-HNE with protein. (*a*) Chemical structures of thet *R*- and *S*-enantiomers of HNE; (*b*) formation of the (*R*,*S*)-HNE–protein Michael adducts, possessing three chiral centres (marked with asterisks). *X* represents the sulfhydryl group of the cysteine residue, the imidazole group of the histidine residue and the ε-amino group of the lysine residue.

chiral centres at C-2, C-4 and C-5 in the tetrahydrofuran moiety (Fig. 1). The novel monoclonal antibody mAbR310 against (*R*)-HNE-modified keyhole limpet haemocyanin showed the highest affinity for the (*R*)-HNE-treated protein and had a higher affinity for the mixture of 2*R*,4*S*,5*R* and 2*S*,4*S*,5*R* HNE–histidine adduct isomers than for HNE–lysine and HNE–cysteine adducts (Hashimoto *et al.*, 2003). An immunohistochemical study using mAbR310 and anti-(*S*)-HNE-modified protein monoclonal antibody mAbS412 revealed that the (*R*)- and (*S*)-HNE epitopes are differentially distributed in the kidney of rats exposed to Fe^{3+}-NTA (Hashimoto *et al.*, 2003; Toyokuni *et al.*, 1994). Very recently, the bispecific character of mAbR310 against modified protein and DNA and the structure of mAbR310 complexed with antigen were reported (Akagawa *et al.*, 2006). The antigen binds to a hydrophobic pocket in the groove, consisting of six CDRs. Interestingly, the hydrophobic pocket was covered by the heavy-chain CDR3 loop (data not shown). To obtain a better understading of how mAbR310 recognizes the aldehyde-modified DNAs and proteins, an antigen-free structure of mAbR310 is necessary. In the present study, we describe the crystallization and preliminary X-ray analysis of antigen-free Fab fragment of mAbR310.

2. Material and methods

2.1. Crystallization and data collection of mAbR310 Fab fragment

We have previously described the preparation and characterization of the monoclonal antibody mAbR310 (Hashimoto *et al.*, 2003) and its Fab fragment (Akagawa *et al.*, 2006). The antibody was cleaved into its Fab and Fc fragments using an ImmunoPure Fab Preparation kit (Pierce). Papain was preactivated with 50 µ*M* cysteine in 2 m*M* ETDA solution. After 30 min activation, the Fab was recovered from the reaction mixture by passing through a protein A column, which effectively retained the Fc fragments and undigested IgG. The Fab fragment was concentrated and further purified by gel filtration using a Superdex 200 10/300 GL (Amersham Biosciences) column equilibrated with 10 m*M* Tris–HCl pH 7.5, 100 m*M* NaCl. The purity of the Fab was checked by both reducing and non-reducing SDS–PAGE (Fig. 2).

Prior to crystallization, the purified mAbR310 Fab was applied onto a HiTrap Desalting 5 ml column (Amersham Pharmacia Biotech) equilibrated with 10 m*M* Tris–HCl pH 7.5 and concentrated to 7.5 mg ml^{-1} using Centricon YM-10 (Millipore). Initial crystallization conditions were screened by the sitting-drop vapour-diffusion method using Crystal Screen I, Crystal Screen II, Low Ionic Strength Screen and Additive Screen (Hampton Research) at 295 K. A 1.0–2.0 µl drop of protein solution was mixed with the same volume of precipitant solution. The crystals were harvested in the reservoir solution and were soaked in trehalose, increasing the concentration stepwise to 25% saturation prior to flash-freezing. Data collection was performed at 98 K. The diffraction data were collected at beamline NW12 of the Photon Factory, Tsukuba, Japan. Diffraction images of the data sets were indexed, integrated and scaled using the *HKL*2000 program suite (Otwinowski & Minor, 1997).

2.2. Phase calculation and refinement

Initial phases were obtained by molecular replacement with the program *MOLREP* from the the *CCP*4 program suite (Collaborative Computational Project, Number 4, 1994). An initial rotation and translation function was calculated using search models derived from mAbR310-homologous antibodies (PDB codes 1ktr, 1i8m, 2jel, 1nqb and 2pcp). Model building in the electron-density map and crystallographic refinement were performed using the *XtalView* program suite (McRee, 1999) and *ARP*/*wARP* (Perrakis *et al.*, 1999).

3. Results and discussion

Only small clustered crystals were obtained in the initial screening. Crystals suitable for X-ray diffraction measurement were obtained by

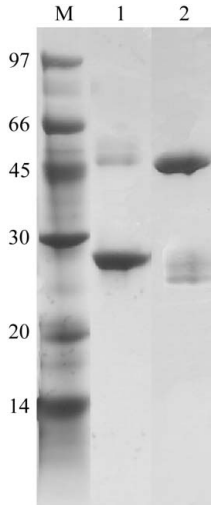

Figure 2
SDS–PAGE of mAbR310 Fab. The gel was electrophoresed with (lane 1) and without (lane 2) β-mercaptoethanol. Lane M, molecular-weight markers (kDa).

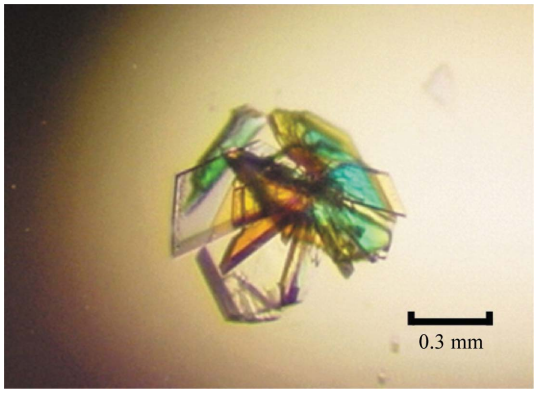

Figure 3
Crystal of mAbR310 Fab (polarizer used).

Table 1
Data-collection statistics.

Values in parentheses are for the highest resolution shell.

Wavelength (Å)	1.0000
Space group	*C*2
Resolution (Å)	28.16–1.84 (1.91–1.84)
Measured reflections	294380
Unique reflections	40218
Completeness (%)	98.7 (94.5)
Mean $I/\sigma(I)$	46.9 (5.8)
$R_{\rm merge}$† (%)	4.9 (20.6)

† $R_{\rm merge} = \sum_{hkl}\sum_i |I_{hkli} - \langle I_{hkl}\rangle|/\sum_{hkl}\sum_i \langle I\rangle hkl\rangle$.

optimization of the conditions and by using additives such as guanidine hydrochloride or divalent cations (Ba^{2+}, Ca^{2+}, Mn^{2+} and Sr^{2+}). The best crystallization condition was obtained with a reservoir solution consisting of 0.1 *M* Na HEPES pH 7.5, 50 m*M* guanidine hydrochloride, 10%(*v*/*v*) 2-propanol and 20%(*w*/*v*) polyethylene glycol 4000. Rhombohedral crystals (0.2 × 0.2 × 0.05 mm; Fig. 3) grew in 7–10 d. The diffraction data were collected from a single crystal using 0.6° oscillations with a crystal-to-detector distance of 175 mm. The crystals diffracted to close to 1.84 Å resolution in space group *C*2, with unit-cell parameters a = 127.04, b = 65.31, c = 64.29 Å, β = 118.88°. Taking the mAbR310 Fab molecular weight to be 46.5 kDa suggests that the crystals contain one molecule of mAbR310 Fab in the asymmetric unit, with a $V_{\rm M}$ of 2.54 Å^3 Da^{-1}, which is within the range given by Matthews (1968). The data-collection statistics are summarized in Table 1. Digestion of the whole antibody molecule using proteases such as papain and ficine gives Fab and Fc fragments. Antigen recognition is carried out by the Fab fragment, which consists of the light chain (V_L and C_L1) and the amino-terminal half of the heavy chain (V_H and C_H1). Fab fragments have a flexible linker region between the variable domains (V_L and V_H) and the constant domains (C_H1 and C_L1), so molecular replacement using a full-length search model was a failure. Recombinant anti-His tag antibody 3d5 (PDB code 1ktr, with only the variable domains) yielded the highest correlation coefficient (0.285) and lowest R factor (0.544) and was used for the next step of the analysis. A search with the constant domains from 2pcp fixing the variable domains yielded the highest correlation coefficient (0.484) and the lowest R factor (0.461). Phase improvement was carried out with the program *ARP*/*wARP* (Perrakis *et al.*, 1999) to generate an electron-density map and an initial model of mAbR310 Fab fragment. Using the program *XtalView* (McRee, 1999), manual refitting of the model was performed. The resulting $2F_o - F_c$ electron-density map showed a clear solvent boundary and reasonable traces of the β-barrel structure of the immunoglobulin fold. Further structural refinements are currently under way. An analysis of the antigen-binding regions of mAbR310 will help to increase our understanding of the molecular mechanisms of chiral selectivity of monoclonal antibodies against HNE-modified proteins.

We thank Drs N. Igarashi, N. Matsugaki and N. Sakabe for data collection. The data collection was approved by the Photon Factory Advisory Committee (Proposals 2005G263 and 2006G177).

References

Akagawa, M., Ito, S., Toyoda, K., Ishii, Y., Tatsuda, E., Shibata, T., Yamaguchi, S., Kawai, Y., Ishino, K., Kishi, Y., Adachi, T., Tsubata, T., Takasaki, Y., Hattori, N., Matsuda, T. & Uchida, K. (2006). *Proc. Natl Acad. Sci. USA*, **103**, 6160–6165.
Benedetti, A., Comporti, M. & Esterbauer, H. (1980). *Biochim. Biophys. Acta*, **620**, 281–296.
Benedetti, A., Pompella, A., Fulceri, R., Romani, A. & Comporti, M. (1986). *Biochim. Biophys. Acta*, **876**, 658–666.
Collaborative Computational Project, Number 4 (1994). *Acta Cryst.* D**50**, 760–763.
Esterbauer, H., Cheeseman, K. H., Dianzani, M. U., Poli, G. & Slater, T. F. (1982). *Biochem. J.* **208**, 129–140.
Esterbauer, H., Schaur, R. J. & Zollner, H. (1991). *Free Radic. Biol. Med.* **11**, 81–128.
Esterbauer, H., Zollner, H. & Scholz, N. (1975). *Z. Naturforsch. C*, **30**, 466–473.
Hashimoto, M., Shibata, T., Wasada, H., Toyokuni, S. & Uchida, K. (2003). *J. Biol. Chem.* **278**, 5044–5051.
Kondo, M., Oya-Ito, T., Kumagai, T., Osawa, T. & Uchida, K. (2001). *J. Biol. Chem.* **276**, 12076–12083.
McRee, D. E. (1999). *J. Struct. Biol.* **125**, 156–165.
Matthews, B. W. (1968). *J. Mol. Biol.* **33**, 491–507.
Okada, K., Wangpoengtrakul, C., Osawa, T., Toyokuni, S., Tanaka, K. & Uchida, K. (1999). *J. Biol. Chem.* **274**, 23787–23793.
Otwinowski, Z. & Minor, W. (1997). *Methods Enzymol.* **276**, 307–326.
Perrakis, A., Morris, R. & Lamzin, V. S. (1999). *Nature Struct. Biol.* **6**, 458–463.
Shacter, E. (2000). *Drug Metab. Rev.* **32**, 307–326.
Stadtman, E. R. & Levine, R. L. (2000). *Ann. NY Acad. Sci.* **899**, 191–208.
Steinberg, D. (1995). *Adv. Exp. Med. Biol.* **369**, 39–48.
Steinberg, D., Parthasarathy, S., Carew, T. E., Khoo, J. C. & Witztum, J. L. (1989). *N. Engl. J. Med.* **320**, 915–924.
Szweda, L. I., Uchida, K., Tsai, L. & Stadtman, E. R. (1993). *J. Biol. Chem.* **268**, 3342–3347.
Toyokuni, S., Uchida, K., Okamoto, K., Hattori-Nakakuki, Y., Hiai, H. & Stadtman, E. R. (1994). *Proc. Natl Acad. Sci. USA*, **91**, 2616–2620.
Toyokuni, S., Yamada, S., Kashima, M., Ihara, Y., Yamada, Y., Tanaka, T., Hiai, H., Seino, Y. & Uchida, K. (2000). *Antioxid. Redox Signal.* **2**, 681–695.
Uchida, K. (2000). *Free Radic. Biol. Med.* **28**, 1685–1696.
Uchida, K. & Stadtman, E. R. (1992). *Proc. Natl Acad. Sci. USA*, **89**, 4544–4548.
Uchida, K. & Stadtman, E. R. (1993). *J. Biol. Chem.* **268**, 6388–6393.